DEPARTMENT OF THE NAVY

DAVID TAYLOR MODEL BASIN

HYDROMECHANICS

○

AERODYNAMICS

○

STRUCTURAL MECHANICS

○

APPLIED MATHEMATICS

THE STRESSES AROUND A RECTANGULAR OPENING WITH ROUNDED CORNERS IN A UNIFORMLY LOADED PLATE

by

S.R. Heller, Jr., J.S. Brock, and R. Bart

STRUCTURAL MECHANICS LABORATORY

RESEARCH AND DEVELOPMENT REPORT

January 1959

Report 1290

DEPARTMENT OF THE NAVY
DAVID TAYLOR MODEL BASIN
WASHINGTON 7, D.C.

IN REPLY REFER TO
S29/12
A9/1
(710:MCC:lkg)
Ser 7-35
17 Feb 1959

'rom: Commanding Officer and Director
'o: Chief, Bureau of Ships (312) (in duplicate)

Subj: NS731-037, Stresses around rectangular openings; forwarding of report on

Encl: (1) TMB Report 1290 entitled, "The Stresses Around a Rectangular Opening with Rounded Corners in a Uniformly Loaded Plate" 11 copies

1. As part of Project NS731-037 the David Taylor Model Basin has been studying stress distributions in the neighborhood of openings. Reports have been published on analytical studies of the stresses around circular and square openings. In enclosure (1) a solution is presented for the stresses around a rectangular opening with rounded corners in a uniformly loaded plate. The numerical cases presented are sufficient to cover most openings found in engineering structures.

2. The investigation is being continued to develop a solution for reinforced openings.

E. E. Johnson

E. E. JOHNSON
By direction

Copy to:
BUSHIPS (106)
(420)
(421)
(440)
(442)
(443)
CHONR, Mech Br (438) (with 2 copies of encl (1))
CO, USN Admin Unit, MIT (with 1 copy of encl (1))
DinC, Webb Inst (with 1 copy of encl (1))

THE STRESSES AROUND A RECTANGULAR OPENING WITH ROUNDED CORNERS IN A UNIFORMLY LOADED PLATE

by

S.R. Heller, Jr., J.S. Brock, and R. Bart

Reprinted from Proceedings of the
Third U.S. National Congress of
Applied Mechanics
held at Brown University
Providence, Rhode Island
June 11-14 1958

January 1959

Report 1290
NS 731-037

THE STRESSES AROUND A RECTANGULAR OPENING WITH ROUNDED CORNERS IN A UNIFORMLY LOADED PLATE

This paper presents a solution for the stresses around a rectangular opening with rounded corners in a uniformly loaded plate. The aspect ratio (length to width) and the radius of curvature of the corners are general. The complex-variable method of Muskhelishvili is used in conjunction with a conformal mapping technique to obtain a solution. Curves showing the tangential stress around the boundary of a typical family of rectangles are presented. In addition, curves are given which show the maximum values of the boundary stress as a function of both aspect ratio and corner radius. The numerical cases are sufficient to cover most openings found in engineering structures.

S. R. Heller, Jr.,
J. S. Brock,
R. Bart
David Taylor Model Basin

Nomenclature

A, B, C, D, E, F = Real coefficients of mapping function
$\left.\begin{matrix} A_n, B_n \\ a_n, b_n \end{matrix}\right\}$ = Complex coefficients of potential functions
h = Height of opening
J_o = Stretch ratio
K = Aspect ratio, h/w
r = Corner radius
$T, \delta T, \lambda T$ = Applied stresses
w = Width of opening
$z = x + iy$
(x,y) = Cartesian coordinates
(α,β) = Orthogonal curvilinear coordinates
γ = Unit circle
$\zeta = e^{\alpha + i\beta}$
ρ = Radius ratio, r/w
$\sigma = e^{i\beta}$
$\left.\begin{matrix} \sigma_x, \sigma_y \\ \sigma_\alpha, \sigma_\beta \end{matrix}\right\}$ = Normal stresses; σ_x is normal to the surface x = constant, etc.
σ_t = Tangential stress at opening
$\tau_{xy}, \tau_{\alpha\beta}$ = Shear stresses
Φ, Ψ = Potential functions of complex variable z
ϕ, ψ = Potential functions of complex variable ζ
_ = Bar above, indicates complex conjugate

Introduction

Since steel cargo ships were first built, the structural arrangements in the vicinity of the large hatches for loading and unloading have been matters of considerable concern. The presence of smaller access openings has caused almost an equal amount of concern. Nor has this interest been confined to ship designers, but, on the contrary, it has been pursued by all designers of plate structures.

The initial theoretical work on this subject was performed by Inglis [1] who approximated the effect of a rectangular opening with rounded corners by a pair of ellipses intersecting obliquely. Savin [2] studied both the square and the rectangle with rounded corners. These two studies, important as they are, have two shortcomings: inaccurate fits—the straight sides as mapped were "sway-backed"—and failure to provide the general solution. Greenspan, working independently and by another method, produced a solution for the square with rounded corners [3] which fails to include a sufficient number of terms. None of the existing solutions has been extended to cover a wide variety of rectangles. The first step in this direction was taken quite recently by Brock who presented a solution [4] for the entire family of squares with rounded corners.

The solution which follows is based on the usual assumptions of plane elasticity: homogeneous, isotropic material within the elastic limit, uniform stress across the thickness of the plate with no stress normal to the plane of the plate, an opening "small" relative to the plate (maximum dimension of the opening < 0.25 plate dimensions), and "small" displacements. The solution is obtained by the complex variable method associated with Muskhelishvili [5].

The Mapping Function

The derivation of the form of the mapping function for rectangular openings may be obtained as follows: Assume a rectangle of unit width and height, K. It is required to map the exterior of the rectangle in the Z-

plane onto the exterior of the unit circle in the ζ-plane. From the stated condition it may be seen from Figure 1 that the vertices of the rectangle are at

$$t = \frac{1}{2}(\pm 1 \pm Ki) \tag{1}$$

The vertices, t, are simply the roots of the expression

$$t^4 - \frac{1}{2}(1 - K^2)\,t^2 + \frac{1}{16}(1 + K^2)^2 = 0 \tag{2}$$

The mapping function may be obtained from the following Schwarz-Christoffel integral

$$Z = Z(\zeta) = A \int_1^{\zeta} \left[t^4 - \frac{1}{2}(1 - K^2)\,t^2 + \frac{1}{16}(1 + K^2)^2 \right]^{\frac{1}{2}} \frac{dt}{t^2} + \text{const.} \tag{3}$$

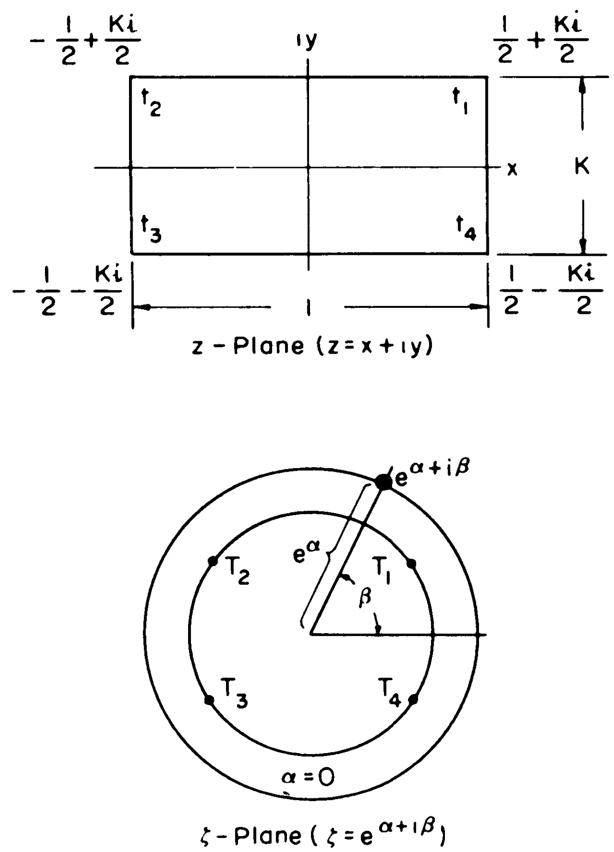

FIGURE 1. CONFORMAL MAP OF A RECTANGULAR OPENING IN THE Z-PLANE ONTO THE UNIT CIRCLE IN THE ζ-PLANE

If we expand the bracket in a descending power series, we obtain

$$Z = A \int_1^{\zeta} \left[t^2 - \frac{1}{4}(1 - K^2) + \frac{1}{8}K^2 t^{-2} + \frac{1}{32}K^2(1 - K^2)\,t^{-4} + \frac{K^2}{128}(1 - 3K^2 + K^4)\,t^{-6} + \dots \right] \frac{dt}{t^2} + \text{const.} \tag{3a}$$

By choosing the arbitrary constant such that no constant term appears in the integral, (3a) becomes

$$Z = A \left[\zeta + \frac{1 - K^2}{4}\frac{1}{\zeta} - \frac{K^2}{24}\frac{1}{\zeta^3} - \frac{K^2(1 - K^2)}{160}\frac{1}{\zeta^5} - \frac{K^2(1 - 3K^2 + K^4)}{896}\frac{1}{\zeta^7} + \dots \right] \tag{4}$$

This expression is the required mapping function in expanded form. This infinite series maps a rectangle, with perfectly straight sides, in the Z-plane onto the unit circle in the ζ-plane. The sides of the rectangle meet at 90° and the radius of curvature at the vertices is not defined. Approximate rectangles with rounded corners may be mapped by retaining only a finite number of terms in (4). Openings with different radii of curvature at the corners may be obtained by changing the number of terms which are retained. A more attractive alternative is to keep a specified number of terms in the series and to permit changes in the coefficients. Thus the form of the mapping function finally suitable to produce rectangular openings with arbitrary aspect ratio and corner radius is given by

$$Z = A\zeta + \frac{B}{\zeta} + \frac{C}{\zeta^3} + \frac{D}{\zeta^5} + \frac{E}{\zeta^7} + \frac{F}{\zeta^9} + \dots \tag{5}$$

The number of terms to be retained and the numerical determination of the constants necessary to obtain a reasonable fit for practical openings, with systematic variation in both aspect ratio and corner radius, will be discussed in another section.

Evaluation of Coefficients in Mapping Function

Expanding (5), setting real and imaginary parts equal, and taking $\alpha = 0$ yields:

$$\begin{aligned} x &= (A + B)\cos\beta + C\cos 3\beta + D\cos 5\beta + E\cos 7\beta + F\cos 9\beta + \dots \\ y &= (A - B)\sin\beta - C\sin 3\beta - D\sin 5\beta - E\sin 7\beta - F\sin 9\beta - \dots \end{aligned} \tag{6}$$

which define the coordinates on the boundary of the opening.

The values assigned these coefficients must assume a reasonable representation of the actual opening. If too many terms are retained, the computation of stress becomes excessively tedious. Conversely, if too few terms are retained, a poor approximation of the actual opening and misleading stress values will result, see [6].

A compromise method was evolved in which the first six values A, B, C, D, E, and F were computed, but only A, B, C, D, and E were used to compute stresses. The conditions imposed on the coefficients were that the curve defined by (6) passes through a given set of points. These are shown in Figure 2. Only one quadrant need be defined because of the periodic character of the circular functions. The values of x and y are:

$$\begin{array}{ll} x_1 = 0.5; & y_1 = 0 \\ x_2 = 0.5 - r(1-\cos\theta_2); & y_2 = 0.5K - r(1-\sin\theta_2) \\ x_3 = 0.5 - r(1-\cos\theta_3); & y_3 = 0.5K - r(1-\sin\theta_3) \\ x_4 = 0.5 - r(1-\cos\theta_4); & y_4 = 0.5K - r(1-\sin\theta_4) \\ & y_5 = 0.5K \\ x_6 = 0; & y_6 = 0.5K \end{array} \qquad (7)$$

where the opening is of unit width, height K, and corner radius r. The coordinate x_5 is not fixed in order to simplify the solution.

Set $\beta_1 = 0$, $\beta_6 = \frac{\pi}{2}$ from symmetry, and let β_5 be known.

Then substituting (7) into (6) yields:

$$\begin{aligned} &A + B + C + D + E + F = 0.5 \\ &(A+B)\cos\beta_m + C\cos 3\beta_m + D\cos 5\beta_m + E\cos 7\beta_m + F\cos 9\beta_m = x_m \\ &(A-B)\sin\beta_m - C\sin 3\beta_m - D\sin 5\beta_m - E\sin 7\beta_m - F\sin 9_m = y_m \\ &(A-B)\sin\beta_5 - C\sin 3\beta_5 - D\sin 5\beta_5 - E\sin 7\beta_5 - F\sin 9\beta_5 = y_5 \\ &A - B + C - D + E - F = 0.5K \\ &m = 2, 3, 4 \end{aligned} \qquad (8)$$

These nine equations contain the six unknown constants A, B, C, D, E, and F and three unknown β's. Note that if a θ_5 had been assumed instead of y_5, an additional unknown β would have been introduced and the necessary tenth equation would have been obtained from x_5.

The choice of the θ's depends on r. For small r, $\theta_2, \theta_3, \theta_4 = 0, \frac{\pi}{4}, \frac{\pi}{2}$ are convenient values. As r approaches $\frac{1}{2}K$, however, this would cause points 1 and 2 to coincide. Alternative values of the θ's were taken as $\frac{\pi}{12}, \frac{\pi}{4}, \frac{\pi}{2}$ and $\frac{\pi}{6}, \frac{\pi}{3}, \frac{\pi}{2}$. In some cases, an average of the coefficients given by two or more such assumptions was found to give a good fit.

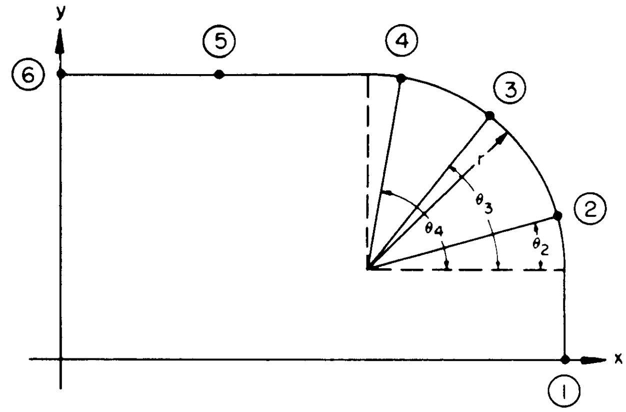

FIGURE 2. POINTS HELD TO DETERMINE MAPPING FUNCTION COEFFICIENTS

The solution of nine simultaneous tracendental equations is by no means simple. It was made feasible by the availability of a desk-size electronic computer on which most of the numerical work was actually carried out. Since a direct solution was impossible, an approximation based on Newton's method was developed. The first and last of Equations (8) were solved for A and B:

$$\left.\begin{aligned} A &= \frac{1}{2}(0.5 + 0.5K) - C - E \\ B &= \frac{1}{2}(0.5 - 0.5K) - D - F \end{aligned}\right\} \qquad (9)$$

These were then substituted into the seven equations obtained from points 2, 3, 4, and 5. A typical example is x_3.

$$C(\cos 3\beta_3 - \cos\beta_3) + D(\cos 5\beta_3 - \cos\beta_3) + E(\cos 7\beta_3 - \cos\beta_3) + F(\cos 9\beta_3 - \cos\beta_3) + 0.5\cos\beta_3 - 0.5 + r(1-\cos\theta_3) = 0 \qquad (10)$$

Assuming that approximate values of C, D, E, F, and β_3 are known, (10) defines a function $f(C, D, E, F, \beta_3)$ which should be equal to zero. If it is not, then the changes required in the values are related by the equation

$$\frac{\partial f}{\partial C}\Delta C + \frac{\partial f}{\partial D}\Delta D + \frac{\partial f}{\partial E}\Delta E + \frac{\partial f}{\partial F}\Delta F + \frac{\partial f}{\partial \beta_3}\Delta\beta_3 + f = 0 \qquad (11)$$

Note that for a single unknown, this would be Newton's iterative method of solution. Since there are seven equations of this form (11), it is clear that the seven quantities ΔC, ΔD, ΔE, ΔF, $\Delta\beta_2$, $\Delta\beta_3$, and $\Delta\beta_4$ can be determined. Whether this results in convergence for the unknowns A, B, C, D, ... depends on complicated algebraic conditions which are beyond the scope of this paper. Actual trial showed that repeated use of (10) and (11) for the seven conditions at 2, 3, 4, and 5 did yield convergent values of the coefficients. The solution of the linear system of equations defined by (11) was carried out automatically by the computer.

The values of the coefficients for the family of openings studied are summarized in Table 1.

It will be noted that Table 1 only includes values of the coefficients for $K \leq 1$. Since the computation process, even with an electronic computer, is tedious, a method utilizing the values from Table 1 to obtain values of the coefficients for $K > 1$ was sought.

Changing only the signs of B and D was found to be a suitable means to rotate the opening 90°. That this simple maneuver is sound is shown in the following:

Let $\qquad B_{ROT} = -B$ and $D_{ROT} = -D$

To get the corresponding point in the first quadrant, take $\beta_{ROT} = \frac{\pi}{2} - \beta$. Hence (6) for the rotated case can be written:

$$x_{ROT} = (A - B)\cos\left(\frac{\pi}{2} - \beta\right) + C\cos 3\left(\frac{\pi}{2} - \beta\right) - D\cos 5\left(\frac{\pi}{2} - \beta\right) + E\cos 7\left(\frac{\pi}{2} - \beta\right)$$

$$y_{ROT} = (A + B)\sin\left(\frac{\pi}{2} - \beta\right) - C\sin 3\left(\frac{\pi}{2} - \beta\right) + D\sin 5\left(\frac{\pi}{2} - \beta\right) - E\sin 7\left(\frac{\pi}{2} - \beta\right) \qquad (6a)$$

which reduces to:

$$x_{ROT} = (A - B)\sin\beta - C\sin 3\beta - D\sin 5\beta - E\sin 7\beta$$

$$y_{ROT} = (A + B)\cos\beta + C\cos 3\beta + D\cos 5\beta + E\cos 7\beta \qquad (6b)$$

Thus, dimensions are preserved, but the opening is rotated 90°. Hence

$$K_{ROT} = \frac{1}{K}, \qquad \rho_{ROT} = \frac{\rho}{K} \qquad (12)$$

Determination of Stress Distribution Caused By Uniform Biaxial Loading

To obtain stresses in problems in plane elasticity using the complex variable method, two potential functions must be determined. These functions can be expressed as:

$$\left.\begin{aligned} \Phi(z) &= \sum_1^K A_n z^n + \sum_1^\infty \frac{a_n}{z^n} \\ \Psi(z) &= \sum_1^K B_n z^n + \sum_1^\infty \frac{b_n}{z^n} \end{aligned}\right\} \qquad (13)$$

where A_n, B_n, a_n, and b_n are constants, possibly complex. The solution is thereby reduced to the evaluation of these constants. The stress condition at the boundary remote from the opening, infinity, will determine A_n and B_n; the stress condition at the other boundary, the opening, will determine a_n and b_n. A_n and B_n, therefore, reflect the type of loading; a_n and b_n, the type of opening.

Following the procedure outlined in [7] which systematized the Muskhelishvili method, stresses are de-

TABLE 1

COEFFICIENTS OF MAPPING FUNCTION

$K = \frac{h}{w}$	$\rho = \frac{r}{w}$	A	B	C	D	E
1/4	1/32	0.35140	0.19775	− 0.03768	− 0.01065	− 0.00123
	1/16	0.34751	0.19455	− 0.03424	− 0.00548	− 0.00077
	3/32	0.34240	0.19195	− 0.02908	− 0.00186	− 0.00082
	1/8	0.33546	0.18773	− 0.02473	+ 0.00002	+ 0.00177
2/7	1/32	0.36395	0.18899	− 0.04176	− 0.01118	− 0.00076
	1/16	0.36007	0.18614	− 0.03802	− 0.00638	− 0.00062
	3/32	0.35502	0.18370	− 0.03283	− 0.00296	− 0.00076
	1/8	0.34859	0.17989	− 0.02834	− 0.00066	+ 0.00118
	1/7	0.34499	0.17788	− 0.02533	+ 0.00122	+ 0.00116

	$\rho = \frac{r}{w}$	A	B	C	D	E
1/3	1/32	0.38036	0.17703	− 0.04696	− 0.01146	− 0.00006
	1/16	0.37653	0.17461	− 0.04288	− 0.00710	− 0.00031
	3/32	0.37157	0.17237	− 0.03764	− 0.00390	− 0.00060
	1/8	0.36625	0.17033	− 0.03187	− 0.00123	− 0.00105
	1/6	0.35730	0.16482	− 0.02550	+ 0.00279	+ 0.00153
2/5	1/32	0.40277	0.15988	− 0.05376	− 0.01135	+ 0.00100
	1/16	0.39907	0.15805	− 0.04929	− 0.00750	+ 0.00023
	3/32	0.39424	0.15611	− 0.04394	− 0.00459	− 0.00030
	1/8	0.38902	0.15419	− 0.03820	− 0.00207	− 0.00082
	5/32	0.38364	0.15239	− 0.03223	− 0.00020	− 0.00141
	3/16	0.37652	0.14791	− 0.02713	+ 0.00368	+ 0.00062
	1/5	0.37391	0.14668	− 0.02469	+ 0.00490	+ 0.00078
1/2	1/32	0.43534	0.13358	− 0.06299	− 0.01042	+ 0.00265
	1/16	0.43193	0.13260	− 0.05805	− 0.00729	+ 0.00112
	3/32	0.42730	0.13112	− 0.05250	− 0.00479	+ 0.00020
	1/8	0.42222	0.12946	− 0.04672	− 0.00251	− 0.00050
	5/32	0.41694	0.12776	− 0.04080	− 0.00037	− 0.00114
	3/16	0.41125	0.12548	− 0.03469	+ 0.00191	− 0.00146
	7/32	0.40440	0.12253	− 0.02812	+ 0.00465	− 0.00127
	1/4	0.39776	0.11997	− 0.02148	+ 0.00730	− 0.00128
2/3	1/32	0.48749	0.08874	− 0.07624	− 0.00764	+ 0.00542
	1/16	0.48477	0.08923	− 0.07070	− 0.00567	+ 0.00260
	3/32	0.48052	0.08859	− 0.06482	− 0.00385	+ 0.00097
	1/8	0.47568	0.08743	− 0.05887	− 0.00201	− 0.00015
	5/32	0.47056	0.08601	− 0.05289	− 0.00014	− 0.00100
	3/16	0.46529	0.08446	− 0.04691	+ 0.00175	− 0.00171
	7/32	0.45996	0.08284	− 0.04092	+ 0.00364	− 0.00237
	1/4	0.45397	0.08118	− 0.03432	+ 0.00475	− 0.00299
	9/32	0.44758	0.08012	− 0.02646	+ 0.00637	− 0.00445
	5/16	0.44112	0.07782	− 0.02000	+ 0.00870	− 0.00445
	1/3	0.43522	0.07581	− 0.01733	+ 0.00837	− 0.00256
1.0	1/32	0.58889	0	− 0.09708	0	+ 0.00819
	1/16	0.58489	0	− 0.09061	0	+ 0.00572
	3/32	0.58071	0	− 0.08414	0	+ 0.00342
	1/8	0.57632	0	− 0.07766	0	+ 0.00134
	5/32	0.57171	0	− 0.07119	0	− 0.00051
	3/16	0.56684	0	− 0.06472	0	− 0.00212
	7/32	0.56169	0	− 0.05825	0	− 0.00344
	1/4	0.55625	0	− 0.05178	0	− 0.00448
	9/32	0.55049	0	− 0.04531	0	− 0.00519
	5/16	0.54440	0	− 0.03883	0	− 0.00556
	11/32	0.53794	0	− 0.03236	0	− 0.00558
	3/8	0.53112	0	− 0.02589	0	− 0.00523
	13/32	0.52392	0	− 0.01942	0	− 0.00450
	7/16	0.51633	0	− 0.01294	0	− 0.00338
	15/32	0.50835	0	− 0.00647	0	− 0.00188
	1/2	0.5	0	0	0	0

termined by

$$\left.\begin{aligned} \sigma_x + \sigma_y &= 2[\Phi'(z) + \overline{\Phi'(z)}] \\ \sigma_y - \sigma_x + 2i\tau_{xy} &= 2[\bar{z}\Phi''(z) + \Psi'(z)] \end{aligned}\right\} \qquad (14)$$

Substitution of (13) into (14) gives:

$$\sigma_x + \sigma_y = 2\left[\sum_1^K (nA_n z^{n-1} + n\bar{A}_n \bar{z}^{n-1}) - \sum_1^\infty \left(\frac{na_n}{z^{n+1}} + \frac{n\bar{a}_n}{\bar{z}^{n+1}}\right)\right]$$

$$\sigma_y - \sigma_x + 2i\tau_{xy} = 2\left\{\sum_1^K [n(n-1)A_n \bar{z} z^{n-2} + nB_n z^{n-1}] + \sum_1^\infty \left[\frac{n(n+1)a_n}{z^{n+2}} - \frac{nb_n}{z^{n-1}}\right]\right\} \qquad (15)$$

Let us now consider the uniform biaxial loading shown in Figure 3. This gives the boundary conditions at infinity:

$$\sigma_x = \lambda T; \quad \sigma_y = T; \quad \tau_{xy} = \delta T \qquad (16)$$

which corresponds to the problem of [4]. From the first of (15), it can be seen that, for $z = \infty$, only positive powers of z are admissible and, specifically, only $n = 1$.

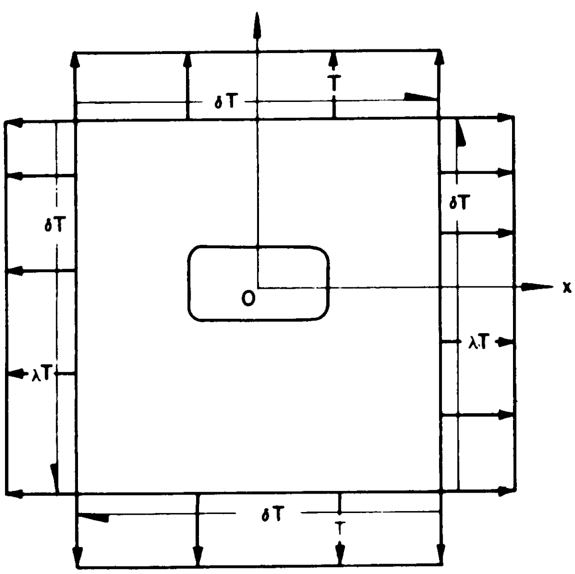

FIGURE 3. UNIFORM BIAXIAL LOAD APPLIED

This gives:

$$A_1 = \bar{A}_1 = \frac{T(1+\lambda)}{4}. \qquad (17a)$$

Similarly, use of the second of (15) also leads to $n = 1$ and yields:

$$B_1 = \frac{T(1-\lambda)}{2} + i\delta T. \qquad (17b)$$

From these values (13), for uniform biaxial loading, becomes:

$$\left.\begin{aligned} \Phi(z) &= \frac{T(1+\lambda)}{4} z + \sum_1^\infty \frac{a_n}{z^n} \\ \Psi(z) &= \frac{T(1-\lambda)}{2} z + i\delta T z + \sum_1^\infty \frac{b_n}{z^n} \end{aligned}\right. \qquad (13a)$$

As pointed out in [8], (13a) are valid for an opening of any shape in an infinite plate subjected to this type of loading.

In order to deal with the stresses at the opening, the following relation* is used:

$$\phi(\sigma) + \frac{z(\sigma)}{\bar{z}'(\bar{\sigma})}\bar{\phi}'(\bar{\sigma}) + \bar{\psi}(\bar{\sigma}) = 0 \qquad (18)$$

where $\sigma = \zeta|_{\alpha=0}$.

This is simply a statement that the opening is a free boundary; i.e., σ_α (normal stress) $= \tau_{\alpha\beta}$ (shear stress) $=$ 0.

The following relations which follow from (5) and (13a) will be useful with (18):

$$\begin{aligned} \phi(\zeta) &= \frac{T(1+\lambda)A}{4}\zeta + \sum_1^\infty \frac{a_n}{\zeta^n} \\ \bar{\phi}'(\bar{\sigma}) &= \frac{T(1+\lambda)A}{4} - \sum_1^\infty n\bar{a}_n \sigma^{n+1} \\ \psi(\zeta) &= \frac{T(1-\lambda)A}{2}\zeta + i\delta TA\zeta + \sum_1^\infty \frac{b_n}{\zeta^n} \\ \bar{\psi}(\bar{\sigma}) &= \frac{T(1-\lambda)A}{2\sigma} - \frac{i\delta TA}{\sigma} + \sum_1^\infty \bar{b}_n \sigma^n \end{aligned} \qquad (19)$$

*[9] pp. 144–145.

$$z(\sigma) = A\sigma + \frac{B}{\sigma} + \frac{C}{\sigma^3} + \frac{D}{\sigma^5} + \frac{E}{\sigma^7}$$

$$\bar{z}'(\bar{\sigma}) = A - \frac{B}{\sigma^2} - \frac{3C}{\sigma^4} - \frac{5D}{\sigma^6} - \frac{7E}{\sigma^8}$$

Substitution of (19) into (18) gives:

$$\phi(\sigma) + \frac{A\sigma^8 + B\sigma^6 + C\sigma^4 + D\sigma^2 + E}{\sigma^7(A - B\sigma^2 - 3C\sigma^4 - 5D\sigma^6 - 7E\sigma^8)} \times \left[\frac{T(1+\lambda)A}{4} - \sum_1^\infty n\bar{a}_n \sigma^{n+1}\right] + \frac{T(1-\lambda)A}{2\sigma} - \frac{i\delta TA}{\sigma} + \sum_1^\infty \bar{b}_n \sigma^n = 0 \quad \text{(18a)}$$

Before further treatment of (18a) it is advantageous to expand the first part of the second term by partial fractions:

$$\frac{A\sigma^8 + B\sigma^6 + C\sigma^4 + D\sigma^2 + E}{\sigma^7(A - B\sigma^2 - 3C\sigma^4 - 5D\sigma^6 - 7E\sigma^8)} = \frac{K_1}{\sigma^7} + \frac{K_2}{\sigma^6} + \ldots + \frac{K_6}{\sigma^2} + \frac{K_7}{\sigma} + \frac{K_8 + K_9\sigma + \ldots + K_{14}\sigma^6 + K_{15}\sigma^7}{A - B\sigma^2 - 3C\sigma^4 - 5D\sigma^6 - 7E\sigma^8} \quad \text{(20)}$$

From which, by clearing fractions and equating coefficients of like powers of σ, is obtained:

$$K_1 = \frac{E}{A}$$

$$K_3 = \frac{D}{A} + \frac{BE}{A^2}$$

$$K_5 = \frac{C}{A} + \frac{BD + 3CE}{A^2} + \frac{B^2E}{A^3} \quad \text{(21)}$$

$$K_7 = \frac{B}{A} + \frac{BC + 3CD + 5DE}{A^2} + \frac{B^2D + 6BCE}{A^3} + \frac{B^3E}{A^4}$$

$$K_2 = K_4 = K_6 = 0$$

K's with larger subscripts are also identifiable but make no contributions to later developments. Hence, (18a) becomes:

$$\phi(\sigma) + \left(\frac{K_1}{\sigma^7} + \frac{K_3}{\sigma^5} + \frac{K_5}{\sigma^3} + \frac{K_7}{\sigma}\right) \times \left[\frac{T(1+\lambda)A}{4} - \sum_1^\infty n\bar{a}_n \sigma^{n+1}\right] + \frac{T(1-\lambda)A}{2\sigma} - \frac{i\delta TA}{\sigma} + \sum_1^\infty \bar{b}_n \sigma^n = 0 \quad \text{(18b)}$$

Multiplication by $d\sigma/2\pi i(\sigma - \zeta)$ and integration around the unit circle, γ, using the Cauchy theorems, gives:

$$-\phi(\zeta) + \frac{T(1+\lambda)A\zeta}{4} - \frac{T(1+\lambda)A}{4}\left(\frac{K_1}{\zeta^7} + \frac{K_3}{\zeta^5} + \frac{K_5}{\zeta^3} + \frac{K_7}{\zeta}\right) + \bar{a}_1\left(\frac{K_1}{\zeta^5} + \frac{K_3}{\zeta^3}\right) + 2\bar{a}_2\left(\frac{K_1}{\zeta^4} + \frac{K_3}{\zeta^2}\right) + 3\bar{a}_3\left(\frac{K_1}{\zeta^3} + \frac{K_3}{\zeta}\right) + 4\bar{a}_4\frac{K_1}{\zeta^2} + 5\bar{a}_5\frac{K_1}{\zeta} - \frac{T(1-\lambda)A}{2\zeta} + \frac{i\delta TA}{\zeta} = 0 \quad \text{(22)}$$ K_5

Successive multiplications, using consecutively higher powers of σ in the numerator, and successive integrations give:

$$-\phi(\zeta) + \frac{T(1+\lambda)A\zeta}{4} + \frac{a_1}{\zeta} - \frac{T(1+\lambda)A}{4}\left(\frac{K_1}{\zeta^7} + \frac{K_3}{\zeta^5} + \frac{K_5}{\zeta^3}\right) + \bar{a}_1\left(\frac{K_1}{\zeta^5} + \frac{K_3}{\zeta^3}\right) + 2\bar{a}_2\left(\frac{K_1}{\zeta^4} + \frac{K_3}{\zeta^2}\right) + 3\bar{a}_3\frac{K_1}{\zeta^3} + 4\bar{a}_4\frac{K_1}{\zeta^2} = 0$$

$$-\phi(\zeta) + \frac{T(1+\lambda)A\zeta}{4} + \frac{a_1}{\zeta} + \frac{a_2}{\zeta^2} - \frac{T(1+\lambda)A}{4}\left(\frac{K_1}{\zeta^7} + \frac{K_3}{\zeta^5} + \frac{K_5}{\zeta^3}\right) + \bar{a}_1\left(\frac{K_1}{\zeta^5} + \frac{K_3}{\zeta^3}\right) + 2\bar{a}_2\frac{K_1}{\zeta^4} + 3\bar{a}_3\frac{K_1}{\zeta^3} = 0$$

(22a)

$$-\phi(\zeta) + \frac{T(1+\lambda)A\zeta}{4} + \frac{a_1}{\zeta} + \frac{a_2}{\zeta^2} + \frac{a_3}{\zeta^3} - \frac{T(1+\lambda)A}{4}\left(\frac{K_1}{\zeta^7} + \frac{K_3}{\zeta^5}\right) + \bar{a}_1\frac{K_1}{\zeta^5} + 2\bar{a}_2\frac{K_1}{\zeta^4} = 0$$

$$-\phi(\zeta) + \frac{T(1+\lambda)A\zeta}{4} + \frac{a_1}{\zeta} + \frac{a_2}{\zeta^2} + \frac{a_3}{\zeta^3} + \frac{a_4}{\zeta^4} - \frac{T(1+\lambda)A}{4}\left(\frac{K_1}{\zeta^7} + \frac{K_3}{\zeta^5}\right) + \bar{a}_1\frac{K_1}{\zeta^5} = 0$$

$$-\phi(\zeta) + \frac{T(1+\lambda)A\zeta}{4} + \frac{a_1}{\zeta} + \frac{a_2}{\zeta^2} + \frac{a_3}{\zeta^3} + \frac{a_4}{\zeta^4} + \frac{a_5}{\zeta^5} - \frac{T(1+\lambda)AK_1}{4\zeta^7} = 0$$

Equating the coefficients of like powers of ζ of (22) and the last of (22a) gives the following system:

$$\begin{aligned}
a_1 &= -\frac{T(1+\lambda)AK_7}{4} + K_5\bar{a}_1 + 3K_3\bar{a}_3 + 5K_1\bar{a}_5 - \frac{T(1-\lambda)A}{2} + i\delta TA \\
a_2 &= 2K_3\bar{a}_2 + 4K_1\bar{a}_4 \\
a_3 &= -\frac{T(1+\lambda)AK_5}{4} + K_3\bar{a}_1 + 3K_1\bar{a}_3 \\
a_4 &= 2K_1\bar{a}_2 \\
a_5 &= -\frac{T(1+\lambda)AK_3}{4} + K_1\bar{a}_1
\end{aligned} \tag{23}$$

Since the K's are real and independent of each other by (21), then

$$a_2 = a_4 = 0 \tag{23a}$$

Separation of the odd a's into their real and imaginary parts for the solution of the remaining Equations (23) leads to:

$$\begin{aligned}
a_1 &= \frac{T}{4}a_1' + i\delta T a_1'' \\
a_3 &= \frac{T}{4}a_3' + i\delta T a_3'' \\
a_5 &= \frac{T}{4}a_5' + i\delta T a_5''
\end{aligned} \tag{23b}$$

where:

$$a_1' = \frac{A\left[(1+\lambda)\left(K_7 + 5K_1K_3 + \dfrac{3K_3K_5}{1-3K_1}\right) + 2(1-\lambda)\right]}{K_5 - 1 + 5K_1^2 + \dfrac{3K_3^2}{1-3K_1}}$$

$$a_1'' = \frac{A}{K_5 + 1 - 5K_1^2 + \dfrac{3K_3^2}{1+3K_1}}$$

$$a_3' = \frac{K_3 a_1' - AK_5(1+\lambda)}{1-3K_1}$$

$$a_3'' = -\frac{K_3 a_1''}{1+3K_1}$$

$$a_5' = K_1 a_1' - AK_3(1+\lambda)$$

$$a_5'' = -K_1 a_1''$$

The single-prime coefficients give the effect of the axial loading; and the double-prime coefficients, the effect of the shear loading. The last of (22a) becomes:

$$\phi(\zeta) = \frac{T}{4}\left[(1+\lambda)A\zeta + \frac{a_1' + 4i\delta a_1''}{\zeta} + \frac{a_3' + 4i\delta a_3''}{\zeta^3} + \frac{a_5' + 4i\delta a_5''}{\zeta^5} - \frac{(1+\lambda)E}{\zeta^7}\right] \tag{24}$$

The usual transformation equation:*

$$\sigma_\alpha + \sigma_\beta = \sigma_x + \sigma_y \tag{25a}$$

plus the knowledge that at a free opening:

$$\begin{aligned}
\sigma_\alpha &= \tau_{\alpha\beta} = 0 \\
\sigma_\beta &= \sigma_t
\end{aligned} \tag{25b}$$

and**

$$\begin{aligned}
\Phi'(z) &= \frac{\phi'(\zeta)}{z'(\zeta)} \\
\Phi'(\bar{z}) &= \frac{\bar{\phi}'(\bar{\zeta})}{z'(\bar{\zeta})}
\end{aligned} \tag{25c}$$

give:

$$\sigma_t = 2\left[\frac{\phi'(\sigma)}{z'(\sigma)} + \frac{\bar{\phi}'(\bar{\sigma})}{\bar{z}'(\bar{\sigma})}\right] = 4\,Re\left[\frac{\phi'(\sigma)}{z'(\sigma)}\right] \tag{26}$$

where "Re" denotes "the real part of."

Substitution of (24) into (26) together with appropriate reduction yields:

$$J_0^2\frac{\sigma_t}{T} = \Delta_0 + \Delta_2\cos 2\beta + \Delta_4\cos 4\beta + \Delta_6\cos 6\beta + 4\delta(N_2\sin 2\beta + N_4\sin 4\beta + N_6\sin 6\beta) \tag{27}$$

where

$$\Delta_0 = (1+\lambda)A^2 + a_1'B + 9a_3'C + 25a_5'D - 49(1+\lambda)E^2$$

$$\Delta_2 = -a_1'A - (1+\lambda)AB + 3a_3'B + 3a_1'C + 15a_5'C +$$

---

*[10], p. 135.

**[7], p. 356.

$$15\,a_3'D - 35(1+\lambda)\,DE + 35\,a_5'E$$

$$\Delta_4 = -3\,a_3'A + 5\,a_5'B - 3(1+\lambda)\,AC - 21(1+\lambda)\,CE + 5\,a_1'D + 21\,a_3'E$$

$$\Delta_6 = -5\,a_5'A - 7(1+\lambda)\,BE - 5(1+\lambda)\,AD + 7\,a_1'E$$

$$N_2 = -a_1''A + 3\,a_3''B - 3\,a_1''C + 15\,a_5''C - 15\,a_3''D - 35\,a_5''E$$

$$N_4 = -3\,a_3''A + 5\,a_5''B - 5\,a_1''D - 21\,a_3''E$$

$$N_6 = -5\,a_5''A - 7\,a_1''E$$

$$J_0^2 = S_0 + S_2 \cos 2\beta + S_4 \cos 4\beta + S_6 \cos 6\beta + S_8 \cos 8\beta$$

where

$$S_0 = A^2 + B^2 + 9\,C^2 + 25\,D^2 + 49\,E^2$$

$$S_2 = -2(AB - 3\,BC - 15\,CD - 35\,DE)$$

$$S_4 = -2(3\,AC - 5\,BD - 21\,CE)$$

$$S_6 = -2(5AD - 7\,BE)$$

$$S_8 = -14\,AE$$

Equation (27) agrees with Greenspan's solution [3] for the ovaloid when $D = E = 0$. Similarly, when $C = D = E = 0$, it agrees with Inglis's solution [1] for the ellipse. If $B = C = D = E = 0$, it also agrees with Kirsch's solution [11] for the circle. Furthermore, when $B = D = 0$, it agrees with Brock's solution [4] for the square with rounded corners.

The definition of stress distribution is not complete, however, until $\psi(\zeta)$ has been determined. To do this, the conjugate of (18) is written:

$$\psi(\sigma) + \overline{\phi}(\overline{\sigma}) + \frac{\overline{z}(\overline{\sigma})}{z'(\sigma)}\,\phi'(\sigma) = 0 \tag{18c}$$

Substitution of (24) and relationships similar to (19) into (18c) followed by treatment similar to that from which (22) and (22a) were developed yields:

$$\psi(\zeta) = \frac{T(1-\lambda)A\zeta}{2} + i\delta TA\zeta + \frac{b_1}{\zeta} + \frac{b_3}{\zeta^3} + \frac{b_5}{\zeta^5} + \frac{7\,T(1+\lambda)\,EK_7}{4\,\zeta^7} \tag{28}$$

where

$$b_1 = \frac{7\,T(1+\lambda)\,EK_1}{4} + K_7 a_1 + 3\,K_3 a_3 + 5\,K_3 a_5 - \frac{T(1+\lambda)\,A}{4}$$

$$b_3 = \frac{7\,T(1+\lambda)\,EK_3}{4} + 3\,K_7 a_3 + 5\,K_3 a_5$$

$$b_5 = \frac{7\,T(1+\lambda)\,EK_5}{4} + 5\,K_7 a_5$$

Numerical Results

Equation (27) gives the stress distribution around the opening for the general case of uniform biaxial loading. Particular interest is centered, however, on the special case of uniform axial tension. Although the computation of stress for this case is somewhat simplified since $\lambda = \delta = 0$, the procedure is typical.

Values of mapping function coefficients for the desired aspect and radius ratios from Table 1 are substituted in (27). The nondimensional stress representation, $\frac{\sigma_t}{T}$, is then calculated for one quadrant, $0 \leq \beta \leq \frac{\pi}{2}$. A sample plot for the family of rectangles with aspect ratio of 1/2 is shown in Figure 4. Also shown is the locus and magnitude of $\frac{\sigma_t}{T}$ maximum.

In addition to the fit of the opening as mapped to the actual opening (calculated points are indicated for β in multiples of 15°), there is also shown in Figure 5 the locus of $\frac{\sigma_t}{T}$ maximum relative to the tangency points of the corner radii. For the sharp corner ($\rho = 0$), the maximum stress occurs at the corner; but, for finite radii, it is located between the midpoint of the fillet and the point of tangency—just as indicated by Inglis [1]—until ρ reaches its limiting value, $\frac{K}{2}$, for which the maximum stress occurs at the juncture of the adjacent corner radii ($\beta = 0$). Thus, as ρ increases, the location of maximum stress at one corner gradually approaches the corresponding point for its adjacent corner and finally reaches it for the limiting value of ρ. Therefore, as ρ increases, there are two effects:

a. A basic reduction in stress concentration with increased radius, and

b. Interaction between stress concentrations (adjacent corners) as the distance between them diminishes. The interaction of two adjacent stress concentrations has been treated by Neuber [12]. In general he shows that, as the two concentrations approach each other, the effect is equivalent to a mutual cancellation or stress relief. On the other hand, for loading along the line of centers of two equal circles (a condition comparable to that discussed herein), Ling [13] shows a different effect. As the circles approach each other, the maximum stress decreases slowly, passes through a minimum where the

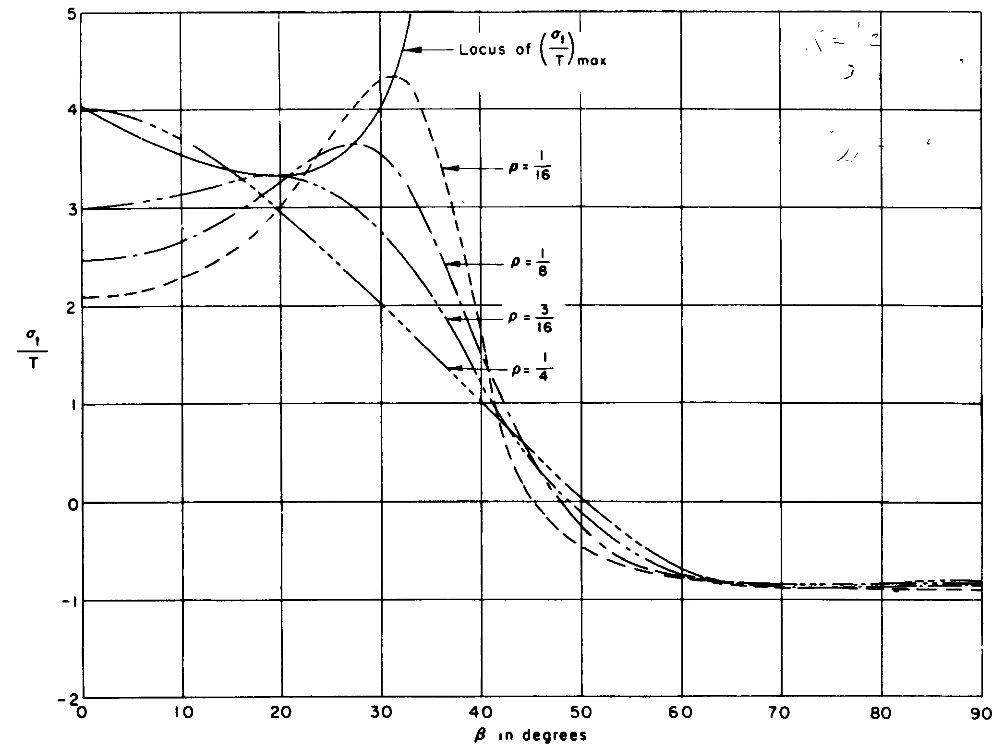

FIGURE 4. TYPICAL TANGENTIAL STRESS DISTRIBUTION AROUND THE BOUNDARY OF ONE QUADRANT, $K = 1/2$

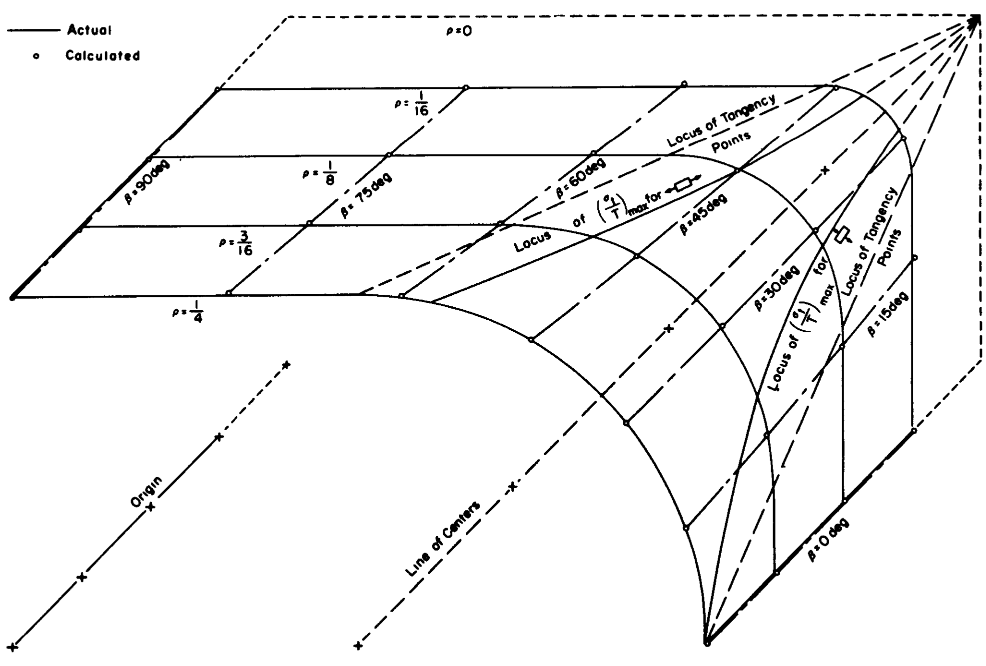

FIGURE 5. COMPARISON OF ACTUAL AND MAPPED OPENINGS, $K = 1/2$

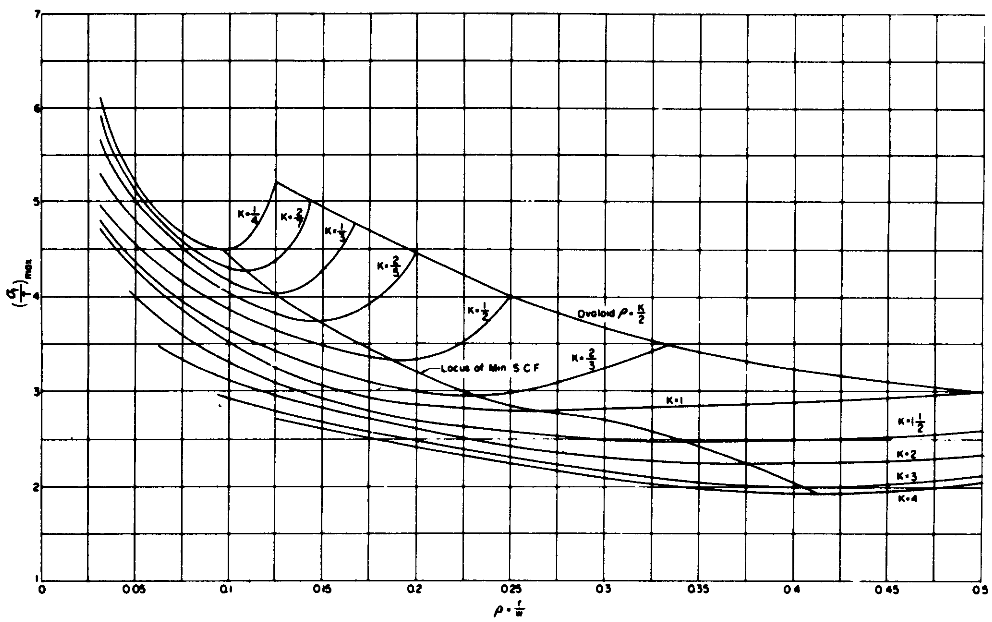

FIGURE 6. MAXIMUM STRESS CONCENTRATION FACTOR VERSUS RADIUS RATIO IN CONTOURS OF ASPECT RATIO

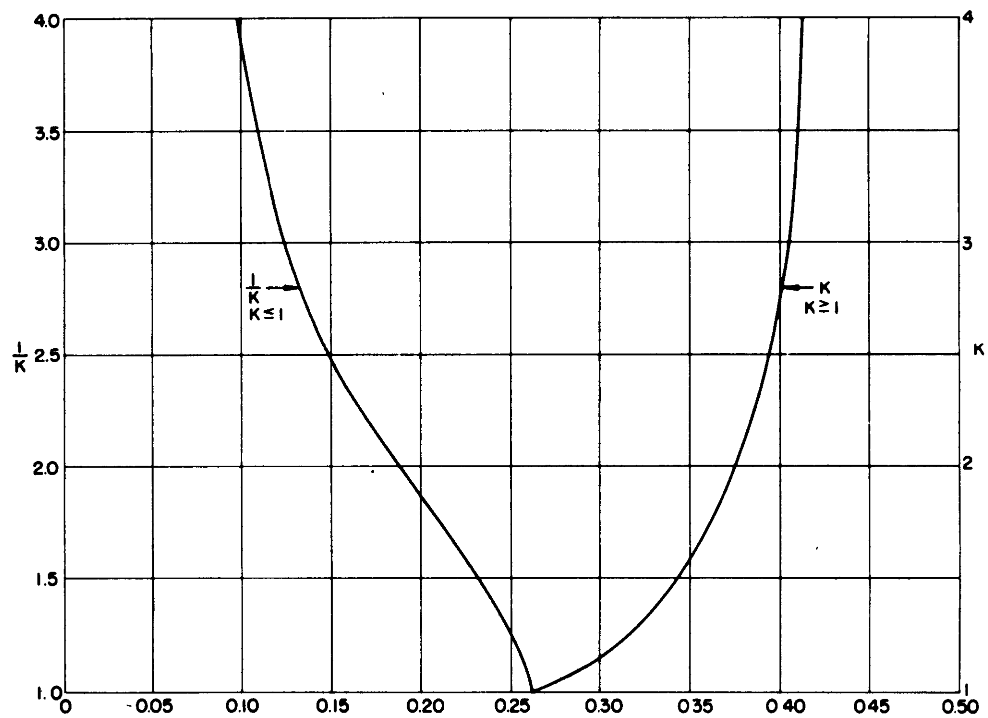

FIGURE 7. RELATION BETWEEN RADIUS AND ASPECT RATIOS FOR MINIMUM STRESS CONCENTRATION FACTOR

circles are tangent, and then rises rapidly to the value for a single circle when the two circles become one.

Thus, as shown in Figure 4, for low values of ρ (corresponding to large separation of the circles) the two effects combine to decrease the maximum stress with increasing radius. For larger values of ρ, corresponding to tangency and then overlapping of the circles in [13], the second effect causes the maximum stress to rise to the limiting value for the ovaloid. The minimum value of $(\sigma_t/T)_{max}$ is attained at ρ greater than that for tangency ($\rho = K/4$) because of the stress reduction obtained from the first effect.

The foregoing discussion has been predicated on cases of loading normal to the long dimension of the rectangle ($K < 1$), but need not be limited to such cases. For tension normal to the short dimension ($K > 1$), the same gradual approach of the location of maximum stress at one corner to its counterpart at the adjacent corner is noted, see Figure 5. Since ρ is limited by the magnitude of the short dimension to a maximum value of 1/2 for $K > 1$, the points of maximum stress at adjacent corners can never coincide. Therefore, for $K > 1$, the interaction effect is less pronounced than for $K < 1$, but is still present.

Plots similar to Figure 4 were made for the series of families of rectangles defined by Table 1 and for the corresponding rotated cases ($K > 1$). These results are summarized in Figure 6 where $(\sigma_t/T)_{max}$ is plotted against ρ in contours of K. It can be seen that, for all families investigated, $(\sigma_t/T)_{max}$ did, in fact, pass through a minimum as ρ increased although the minimum became less pronounced as K increased.

Finally, the most appropriate ρ for a given K, i.e., the ρ for a given K which gives the minimum $(\sigma_t/T)_{max}$, is shown in Figure 7. The ordinates of Figure 7 were deliberately chosen as $1/K$ for $K \leq 1$ and K for $K \geq 1$ to coincide with the usual expression of the ratio of the sides of a rectangle as a number greater than unity.

Acknowledgments

The authors wish to express their sincere appreciation to the Bureau of Ships, Navy Department, for sponsoring the research embodied in this paper. The opinions or assertions contained herein are those of the authors and do not necessarily reflect the official opinion of the Department of the Navy or the naval establishment at large. They also desire to extend their gratitude to Mrs. Mildred R. Overby who carefully and meticulously performed and checked the many tedious calculations on which Figure 6 is based.

Bibliography

1. Inglis, C. E., "Stresses in a Plate due to the Presence of Cracks and Sharp Corners," Trans. Inst. Nav. Arch., vol. 55, 1913, pp. 219–230.

2. Savin, G. N., "Spannungserhöhung am Rande von Löchern," VEB Verlag Technik, Berlin, 1956.

3. Greenspan, M., "Effect of a Small Hole on the Stresses in a Uniformly Loaded Plate," Quart. Appl. Math., vol. 2, No. 1, 1944, pp. 60–71.

4. Brock, J. S., "Analytical Determination of the Stresses Around Square Holes with Rounded Corners," DTMB Report 1149, Nov., 1957.

5. Muskhelishvili, N. I., "Some Basic Problems of the Mathematical Theory of Elasticity," (translation by J. R. M. Radok), P. Noordhoff, Ltd., Groningen, Holland, 1953.

6. Kikukawa, M., "On a Method of Calculating Stress Concentration in an Infinite Plate with a Hole of Arbitrary Profile," Proc. 1st Japan Nat. Cong. for Appl. Mech., 1951, pp. 185–191.

7. Joseph, J. A. and Brock, J. S., "The Stresses Around a Small Opening in a Beam Subjected to Pure Bending," Jour. Appl. Mech., vol. 17, No. 4, 1950, pp. 353–358.

8. Morkovin, V., Discussion of Reference 3, Quart. Appl. Math., vol. 2, No. 4, 1944, pp. 350–352.

9. Sokolnikoff, I. S., "Mathematical Theory of Elasticity," (mimeographed lecture notes), Brown University, Providence, R. I., 1941.

10. Coker, E. G. and Filon, L. N. G., "A Treatise on Photoelasticity," Cambridge University Press, London, 1931.

11. Kirsch, G., "Die Theorie der Elastizität und die Bedürfnisse der Festigkeitslehre," Zeit, V. D. I., vol. 42, No. 29, 1898, pp. 797–807.

12. Neuber, H., "Theory of Notch Stresses: Principles for Exact Stress Calculation," DTMB Translation 74, Nov. 1945.

13. Ling, C. B., "Stresses in a Plate with Two Equal Holes," Jour. Appl. Phys., vol. 19, No. 1, 1948, pp. 77–82.

INITIAL DISTRIBUTION

Copies

11 CHBUSHIPS, Library (Code 312)
- 5 Tech Library
- 1 Tech Asst to Chief (Code 106)
- 1 Prelim Des Br (Code 420)
- 1 Prelim Des Sec (Code 421)
- 1 Hull Des (Code 440)
- 1 Sci & Res (Code 442)
- 1 Structure (Code 443)

2 CHONR, Mech Br (Code 438)

1 CO, USN Admin Unit, MIT, Cambridge, Mass.

1 Administrator, Webb Inst of Nav Arch, Glen Cove, L.I., N.Y.

David Taylor Model Basin. Report 1290.
THE STRESSES AROUND A RECTANGULAR OPENING WITH ROUNDED CORNERS IN A UNIFORMLY LOADED PLATE, by S.R. Heller, Jr., J.S. Brock, and R. Bart. January 1959. 13p. illus., graphs, tables, refs. UNCLASSIFIED

This paper presents a solution for the stresses around a rectangular opening with rounded corners in a uniformly loaded plate. The aspect ratio (length to width) and the radius of curvature of the corners are general. The complex-variable method of Muskhelishvili is used in conjunction with a conformal mapping technique to obtain a solution. Curves showing the tangential stress around the boundary of a typical family of rectangles are presented. In addition, curves are given which show the maximum values of the boundary stress as a function of both aspect ratio and corner radius. The numerical cases are sufficient to cover most openings found in engineering structures.

1. Plates – Stresses – Mathematical analysis
I. Heller, Samuel R.
II. Brock, Joseph S.
III. Bart, Robert
IV. NS 731-037

David Taylor Model Basin. Report 1290.
THE STRESSES AROUND A RECTANGULAR OPENING WITH ROUNDED CORNERS IN A UNIFORMLY LOADED PLATE, by S.R. Heller, Jr., J.S. Brock, and R. Bart. January 1959. 13p. illus., graphs, tables, refs. UNCLASSIFIED

This paper presents a solution for the stresses around a rectangular opening with rounded corners in a uniformly loaded plate. The aspect ratio (length to width) and the radius of curvature of the corners are general. The complex-variable method of Muskhelishvili is used in conjunction with a conformal mapping technique to obtain a solution. Curves showing the tangential stress around the boundary of a typical family of rectangles are presented. In addition, curves are given which show the maximum values of the boundary stress as a function of both aspect ratio and corner radius. The numerical cases are sufficient to cover most openings found in engineering structures.

1. Plates – Stresses – Mathematical analysis
I. Heller, Samuel R.
II. Brock, Joseph S.
III. Bart, Robert
IV. NS 731-037

David Taylor Model Basin. Report 1290.
THE STRESSES AROUND A RECTANGULAR OPENING WITH ROUNDED CORNERS IN A UNIFORMLY LOADED PLATE, by S.R. Heller, Jr., J.S. Brock, and R. Bart. January 1959. 13p. illus., graphs, tables, refs. UNCLASSIFIED

This paper presents a solution for the stresses around a rectangular opening with rounded corners in a uniformly loaded plate. The aspect ratio (length to width) and the radius of curvature of the corners are general. The complex-variable method of Muskhelishvili is used in conjunction with a conformal mapping technique to obtain a solution. Curves showing the tangential stress around the boundary of a typical family of rectangles are presented. In addition, curves are given which show the maximum values of the boundary stress as a function of both aspect ratio and corner radius. The numerical cases are sufficient to cover most openings found in engineering structures.

1. Plates – Stresses – Mathematical analysis
I. Heller, Samuel R.
II. Brock, Joseph S.
III. Bart, Robert
IV. NS 731-037

David Taylor Model Basin. Report 1290.
THE STRESSES AROUND A RECTANGULAR OPENING WITH ROUNDED CORNERS IN A UNIFORMLY LOADED PLATE, by S.R. Heller, Jr., J.S. Brock, and R. Bart. January 1959. 13p. illus., graphs, tables, refs. UNCLASSIFIED

This paper presents a solution for the stresses around a rectangular opening with rounded corners in a uniformly loaded plate. The aspect ratio (length to width) and the radius of curvature of the corners are general. The complex-variable method of Muskhelishvili is used in conjunction with a conformal mapping technique to obtain a solution. Curves showing the tangential stress around the boundary of a typical family of rectangles are presented. In addition, curves are given which show the maximum values of the boundary stress as a function of both aspect ratio and corner radius. The numerical cases are sufficient to cover most openings found in engineering structures.

1. Plates – Stresses – Mathematical analysis
I. Heller, Samuel R.
II. Brock, Joseph S.
III. Bart, Robert
IV. NS 731-037

David Taylor Model Basin. Report 1290.
THE STRESSES AROUND A RECTANGULAR OPENING WITH ROUNDED CORNERS IN A UNIFORMLY LOADED PLATE, by S.R. Heller, Jr., J.S. Brock, and R. Bart. January 1959. 13p. illus., graphs, tables, refs. UNCLASSIFIED

This paper presents a solution for the stresses around a rectangular opening with rounded corners in a uniformly loaded plate. The aspect ratio (length to width) and the radius of curvature of the corners are general. The complex-variable method of Muskhelishvili is used in conjunction with a conformal mapping technique to obtain a solution. Curves showing the tangential stress around the boundary of a typical family of rectangles are presented. In addition, curves are given which show the maximum values of the boundary stress as a function of both aspect ratio and corner radius. The numerical cases are sufficient to cover most openings found in engineering structures.

1. Plates – Stresses – Mathematical analysis
I. Heller, Samuel R.
II. Brock, Joseph S.
III. Bart, Robert
IV. NS 731-037

David Taylor Model Basin. Report 1290.
THE STRESSES AROUND A RECTANGULAR OPENING WITH ROUNDED CORNERS IN A UNIFORMLY LOADED PLATE, by S.R. Heller, Jr., J.S. Brock, and R. Bart. January 1959. 13p. illus., graphs, tables, refs. UNCLASSIFIED

This paper presents a solution for the stresses around a rectangular opening with rounded corners in a uniformly loaded plate. The aspect ratio (length to width) and the radius of curvature of the corners are general. The complex-variable method of Muskhelishvili is used in conjunction with a conformal mapping technique to obtain a solution. Curves showing the tangential stress around the boundary of a typical family of rectangles are presented. In addition, curves are given which show the maximum values of the boundary stress as a function of both aspect ratio and corner radius. The numerical cases are sufficient to cover most openings found in engineering structures.

1. Plates – Stresses – Mathematical analysis
I. Heller, Samuel R.
II. Brock, Joseph S.
III. Bart, Robert
IV. NS 731-037